Swelling kinetics of a compressed lamellar phase

Jacques Leng, Frédéric Nallet, Didier Roux

Eur. Phys. J. E **4**, 77–83 (2001)

THE EUROPEAN PHYSICAL JOURNAL E

EDP Sciences

Swelling kinetics of a compressed lamellar phase

J. Leng[a], F. Nallet, and D. Roux

Centre de recherche Paul-Pascal, CNRS, Av. Schweitzer, F-33600 Pessac, France

Received 25 May 2000 and Received in final form 4 August 2000

This article is dedicated to Marc Leng

Abstract. We investigate how multilamellar vesicles prepared in a compressed state under flow return to equilibrium. The kinetics is studied by following the temporal evolution of the viscoelasticity after the shear is stopped. It exhibits a two-step relaxation whose slower stage is strongly affected by temperature. According to a simple model, the temperature-dependent permeability of the lamellar phase is deduced from the measurements. We propose to attribute the permeability to handle-like defects, and its temperature dependence to an increase of the defect density when the lamellar-to-sponge phase transition is approached.

PACS. 05.70.Ln Nonequilibrium and irreversible thermodynamics – 61.30.Jf Defects in liquid crystals – 83.70.Hq Heterogeneous liquids: suspensions, dispersions, emulsions, pastes, slurries, foams, block copolymers, etc.

1 Introduction

It has been recently shown that the effect of shear on lyotropic lamellar (L_α) phases can be described using an *orientation diagram* [1]. As a generalisation of equilibrium phase diagrams, the orientation diagram maps the shear-induced (steady) textures as a function of a dynamic parameter—usually the shear rate—and a thermodynamic parameter—*e.g.*, the volume fraction of membranes. By increasing the shear rate, one commonly encounters three steady states: at very low shear rate (typically $\dot\gamma < 1\ \mathrm{s}^{-1}$, depending on concentration) a partially oriented state with the normal to the smectic layers parallel to the shear gradient; at intermediate shear rates ($1 < \dot\gamma < 500\ \mathrm{s}^{-1}$), the membranes roll up onto themselves to form multilamellar, monodisperse and close-packed vesicles—the so-called *onion texture*; at even higher shear rates, one gets back-oriented membranes. These various organisations are separated by dynamic transitions which were characterised using rheology [2,3]. It is important to note that although quite general [4,5], this behaviour is not universal and remains very system-dependent [6–8]. Moreover, the mechanism of onions formation is still under a theoretical debate [9,10].

The *onion texture* is fascinating in many aspects. For instance, it offers a unique way to control perfectly the texture of the lamellar phase on macroscopic scales. Typically of order of 1 μm, the size of the multilamellar vesicles is fixed by the shear rate and follows a power law ($R \sim \dot\gamma^{-1/2}$) as measured by small-angle light scattering [1] (this power law appears to be somewhat system-dependent). Some characteristics of the vesicular state on properties of L_α phases were given using conductivity [11] and viscoelasticity [12].

Recently, the opportunity to control additionally the spatial organisation of the onions was demonstrated [13–15]. Indeed, for one particular L_α phase a series of dynamic transitions leads to a population of shear-ordered onions, in a close analogy with the shear ordering of concentrated colloidal suspensions [16]. The resultant texture consists of hexagonal planes of onions sliding on each other under flow and referred to as the *layered state* of onions.

In this article, we focus our attention on a very peculiar onion regime where the vesicles are nonetheless well ordered but also *compressed* under flow. This state is evidenced by combining several experimental observations (light scattering, neutron scattering, etc.) and consists of large multilamellar vesicles which, under flow, have expelled some of their inner water. We use this opportunity to investigate the *relaxation* processes of the compressed vesicles once the shear is stopped. Studied by means of viscoelasticity, the kinetics exhibits a two-step process: whereas the first stage is relatively fast ($\tau \approx 100$ s) and, as a consequence not well resolved using rheology alone, the second stage is much slower ($\tau \approx 0.5$–3 hours). It is also *strongly dependent* upon the working temperature. We attribute this second stage to the swelling of the vesicles by the expelled water. According to a simple diffusion model for the membrane displacement, we deduce from the slow kinetics the *permeability* of the lamellar phase. We find that it strongly increases when temperature is raised. We

[a] *Present address*: Department of Physics and Astronomy, The University of Edinburgh, Kings' Buildings, Mayfield road, JCMB, Edinburgh EH9 3JZ, UK. e-mail: `leng@ph.ed.ac.uk`

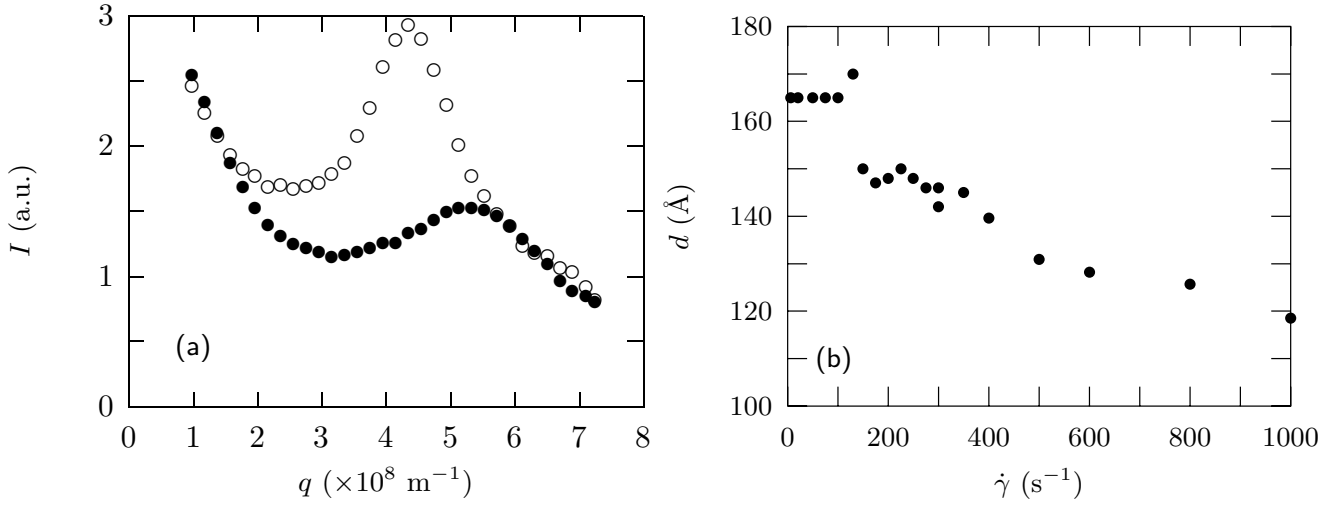

Fig. 1. (a) Modification of the small-angle neutron scattering profile of the L_α phase under shear below ($\circ$ $\dot{\gamma} = 50$ s^{-1}) and above ($\bullet$ $\dot{\gamma} = 400$ s^{-1}) the jump-of-size transition ($T = 28°$C). (b) Evolution of the smectic period as a function of the shear rate measured by SANS under shear ($T = 28°$C).

propose to correlate this last effect to the proliferation, close to the lamellar-to-sponge phase transition, of handle-like defects [11] connecting the membranes.

2 The state of compressed onions

The L_α phase we studied is a quaternary mixture of sodium-dodecyl sulfate, octanol and brine (7%, 8%, 85% w/w, respectively, NaCl at 20 g/l) whose phase diagram has already been published [17]. This L_α phase is stabilised by steric interactions [18] and its smectic period is $d \approx 160$ Å for this composition. At equilibrium, the system undergoes a lamellar-to-sponge phase transition when the temperature is raised around $T \approx 31°$C.

The orientation diagram was studied in the plane $(T, \dot{\gamma})$ [14,19]. One distinguishes two regimes depending on the temperature. At low temperature ($T < 26°$C), the sequence of membrane organisations is the following: at very low shear rate ($\dot{\gamma} < 1$ s^{-1}), the membranes are preferentially oriented in the direction of the flow; at a first critical shear rate ($\dot{\gamma} \approx 1$ s^{-1}), the phase undergoes the lamellar-to-onion transition; above a second critical shear rate ($\dot{\gamma} \approx 50$ s^{-1}), the onions get spontaneously ordered (*layered onions*). The transition only reorganizes the spatial locations of the onions from an amorphous (the local order that does not extend further than typically the third neighbour) to a more ordered state, without any change in the onion size. Finally, one retrieves oriented membranes above a third critical shear rate (note, however, that the shear values at the transition depend on T [14, 19]). At high temperature ($26 < T < 31°$C), the sequence is analogous, apart from the high shear rate regime. Instead of oriented membranes, a new transition takes place (the *jump-of-size* transition) whose main features are the following:

1) at the transition the size of the onions increases discontinuously from 1 to 10 μm typically and then *does not depend any more* on the shear rate [14];
2) the transition is accompanied with a decrease of the smectic period of the lamellar phase [13].

The second point is shown in Figure 1(a) where we display the modification of the small-angle neutron scattering (SANS) profiles (spectrometer PAXY, Laboratoire Léon-Brillouin, laboratoire commun CEA-CNRS, Saclay, France) under shear, below and above the jump-of-size transition. Below the transition, there is no noticeable effect of shear on the SANS profile. Above the transition, the Bragg peak of the smectic stacking is shifted towards higher wave vectors than the equilibrium one, which corresponds to smaller smectic distances. The systematic study as a function of the shear rate leads to Figure 1(b) where we see that d decreases continuously with $\dot{\gamma}$ above the jump-of-size transition. Meanwhile, the numerous Bragg spots of the small-angle light scattering patterns [13] not only show that the onions still exist but also that they are extremely well ordered under shear.

The combination of these results (light+neutron scattering) suggests that the onions have expelled some of the inner water and subsequently this state will be referred to as *compressed onions*. While not proven, it was argued in reference [13] that the shear rate—usually fixing the size of the vesicles (through a mechanism where the viscous stress is balanced against the energetical cost of making a vesicle [1])—now acts as a compression force. This could be the reason why the size of the vesicles does not depend anymore on the shear rate and, instead, the shear rate controls the compression.

It is also possible to evidence this compressed state using macroscopic techniques instead of small-angle neutron scattering. Let us first recall that at least two paths of the orientation diagram may lead to the compressed state of onions. For instance, one can either work at constant

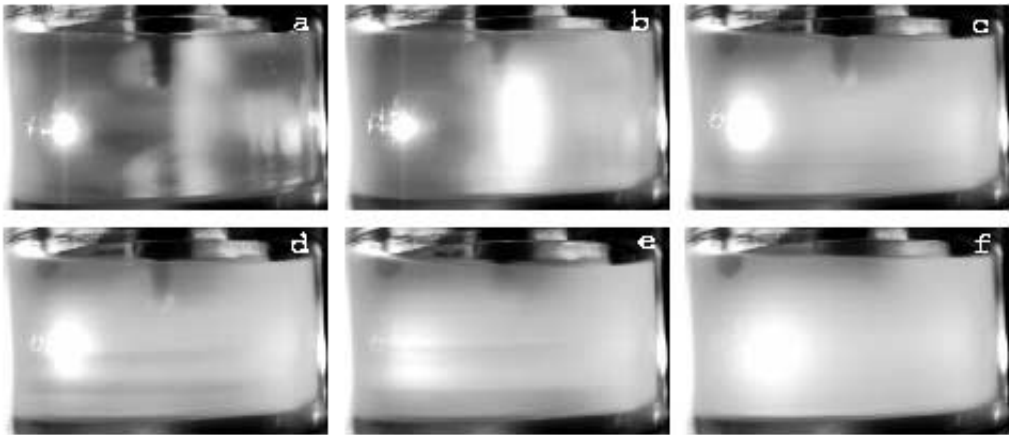

Fig. 2. Optical visualisation in a transparent Couette cell of the jump-of-size transition induced by a step of temperature from oriented membranes (a) to big and compressed onions (f) ($T = 17 \rightarrow 27°\mathrm{C}$, $\dot{\gamma} = 1000\ \mathrm{s}^{-1}$). Images (a) and (f) correspond to the respective steady states whereas images (b)–(e) describe the transient states. Note the difference of optical contrast between images (a) and (f) and a peculiar transient state with horizontal bands (d).

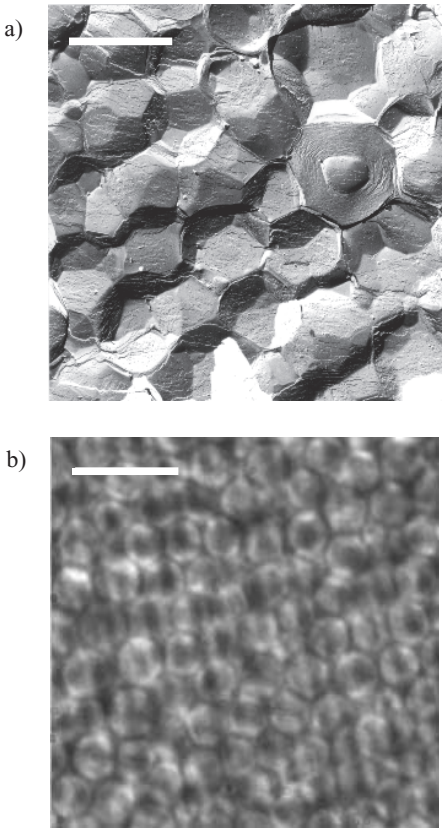

Fig. 3. (a) Freeze-fracture electron micrograph of a "regular" onion texture: vesicles are in a close contact and fill up completely the space [17]. The bar represents 5 μm. (b) Optical observation of the texture of *compressed* onions under a microscope with partially crossed polarizers once the shear is stopped. One clearly sees the vesicles as well as the "free space" between them corresponding to the expelled water. The bar represents 20 μm.

temperature ($T > 26°\mathrm{C}$) and carry out a jump of shear rate from small layered onions to big compressed onions, or one can work at constant shear rate (high shear rate regime $\dot{\gamma} > 500\ \mathrm{s}^{-1}$) and use a jump of temperature to go from oriented membranes to big compressed onions. We display in Figure 2 the optical aspect of the sample under flow during the latter process. A camera records the images taken from a transparent Couette cell mounted on a rheometer (Carrimed CSL100). A laser beam is sent through the cell in order to observe the diffusion/diffraction patterns resulting from shear-induced structures, if any. The most interesting result is the flagrant difference between the state of oriented membranes (Fig. 2(a)) and the state of compressed onions under shear (Fig. 2(f)). The latter offers a very turbid liquid which scatters multiply the light. This is not the case neither for oriented membranes nor for the usual onion texture.

We attribute this effect to the creation of an *in-out* (or *onions-water*) optical contrast which does not exist when the onions are not compressed (Fig. 3). Indeed, the nature of the optical contrast evolves through the expulsion of water; for relaxed, swollen onions the constrast (most probably) originates from the birefringence of the L_α phase itself (with a difference of refractive indexes $\Delta n = n_\mathrm{o} - n_\mathrm{e} \approx 10^{-2}$ [1]), whereas compressed onions exhibit a more pronounced variation of refractive indexes: $\Delta n = n_{L_\alpha} - n_\mathrm{water} \approx 10^{-1}$. When the shear is stopped, the turbidity slowly disappears (in a time typically comparable to the lifetime of the slow relaxation in viscoelasticity measurements) and one recovers a transparent sample similar to the one displayed in Figure 2(a). This simple picture corroborates the description in terms of compressed onions.

The question to describe how onions get compressed is not addressed here. We simply propose to correlate the flow mechanism to the compression. Indeed, the small-angle light scattering indicates that onions are spatially

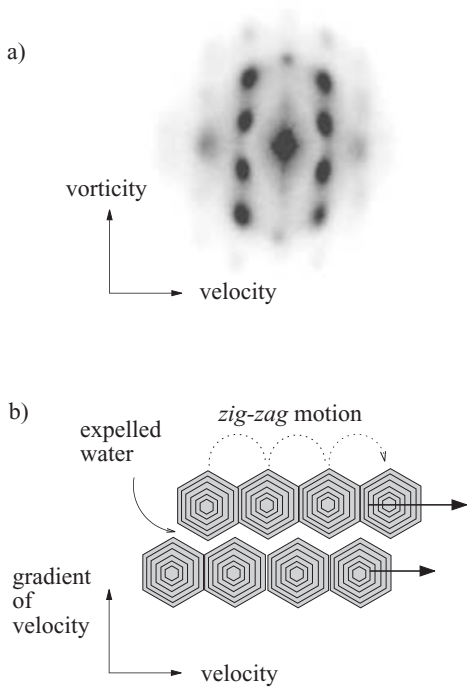

Fig. 4. (a) Small-angle light scattering pattern obtained *in situ* in a Couette cell. (b) Naïve drawing of the flow mechanism for big and compressed onions. In order to flow, the hexagonal planes (side view) have to "jump" from one crystallographic position to a neighboring one. This probably induces a compression of the soft vesicles that expel some of the inner water.

correlated under shear (Fig. 4). They are located on hexagonal planes that slip past each other under flow. The situation is quite similar to the shear ordering of concentrated suspensions and the flow mechanism presumably consists of the so-called *zig-zag* motion [20]. In this situation, and because the onions are soft vesicles, one can imagine that the compression originates from the necessary passage from one "crystallographic" position to another (Fig. 4). We consequently expect that the water which is expelled comes in between the shear planes of onions to "lubricate" their motion.

3 The swelling kinetics

In the rest of this article, we investigate the relaxation processes of the compressed vesicles just after the shear is stopped. The first thing important to notice is that, though there are important changes in the light scattering spectra all along the relaxation processes, there is no *quantitative* evolution, in the sense that the Bragg spots remain fixed in reciprocal space: the underlying "lattice" is apparently not modified during the solvent intake. On the other hand, the smectic period that is diminished under flow increases back when shear is stopped to restore its equilibrium value d_0 [21]. Here, we study the swelling

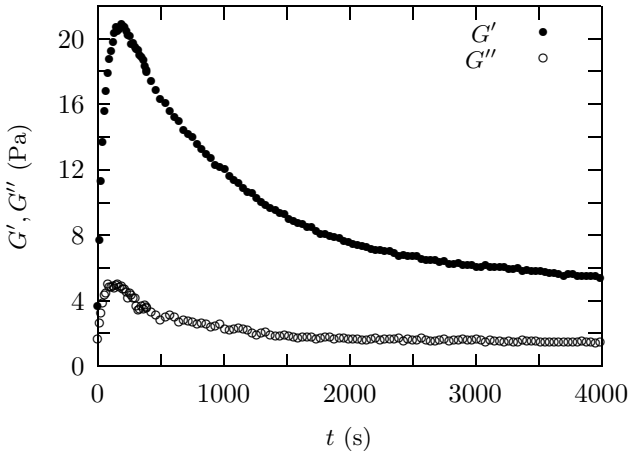

Fig. 5. Relaxation kinetics of the storage and loss moduli G' and G''. A stationary state of compressed onions ($\sigma_p = 15$ Pa, $T_p = 26°$C) has been prepared and the flow abruptly stopped at $t = 0$.

kinetics by means of viscoelasticity. The onions are prepared in a stress-controlled rheometer (Carrimed CSL100) equipped with a home-made transparent Mooney-Couette cell (Fig. 2). The cell is made of plexiglass (poly-methylmethacrylate) and is thermostated within 0.1°C of accuracy. The compressed onions are prepared by applying a constant stress σ_p (at a controlled temperature T_p) until a stationary state is reached (as monitored by the temporal evolution of the viscosity). Then, the stress is abruptly stopped and one records the temporal evolution of the storage and loss moduli G' and G'' at a frequency $f = 1$ Hz and for a relative strain $\gamma = 1\%$ (checked to be within the linear response regime). A characteristic result describing such an experiment is given in Figure 5. When the shear is stopped ($t = 0$ s), the moduli exhibit a two-step relaxation with very different behaviours and characteristic times. Whereas the first stage corresponds to a fast increase of the two moduli ($\tau \approx 100$ s), the second process is much slower ($\tau \approx 1$ hour) and leads to a finite value of the moduli (which was shown to depend on the microstructure [12]). As mentioned above, one observes that the shear-induced turbidity decreases with time, following the slower process. Indeed, the sample becomes transparent again only at the end of the second elastic relaxation. We deduce from such a result that the second step of the relaxation is related to the swelling kinetics of the vesicles. This idea has been confirmed by a preliminary study of time-resolved X-ray scattering (beamline ID02A, ESRF, Grenoble) where we observed that the smectic period slowly increases in the second stage of the kinetics to finally reach its equilibrium value d_0 [22].

We have tested experimentally the influence of the stress of preparation σ_p on this kinetics: it has no influence on the two characteristic times. In contrast, the temperature strongly affects the kinetics. To study this effect, we can use two different strategies. The first one consists in generating the compressed onions with the parameters (σ_p, T_p), to analyse the kinetics and to study it again for

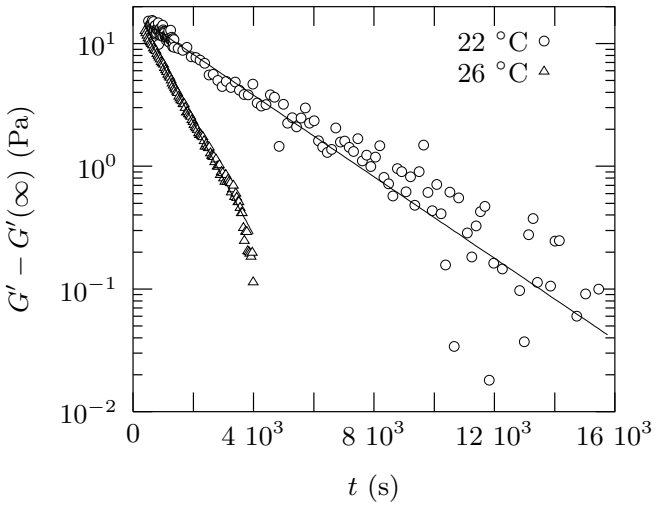

Fig. 6. Relaxation kinetics of the reduced storage modulus $G'(t) - G'(\infty)$ for two temperatures, in a semi-log scale. The behaviour is almost mono-exponential and the full lines are the best fits according to a single exponential process. Note how the kinetics is slowed down when the temperature is lowered. (Onions prepared at $\sigma_p = 15$ Pa, $T = 26°$C.)

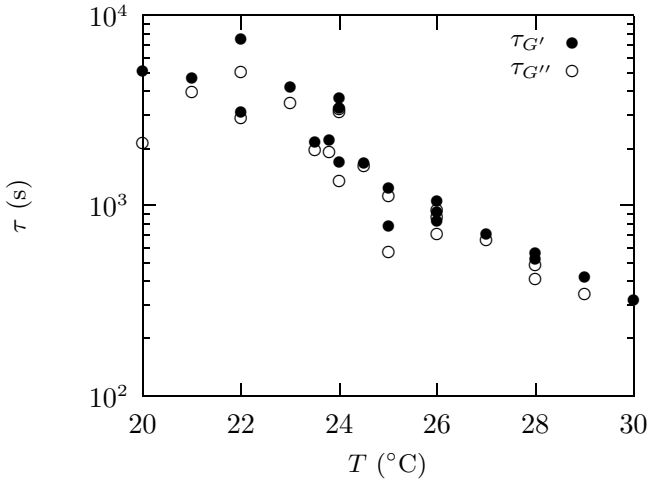

Fig. 7. Characteristic time of the swelling kinetics as a function of the temperature, as deduced from a single-exponential fit of the slow stage of the kinetics.

onions generated with other parameters (σ_p', T_p'). Doing so, we not only modify the temperature but accordingly the size of the vesicles (which is mainly fixed by the preparation temperature [14]). That is why we have chosen to keep constant the temperature of preparation T_p and to make a jump of temperature ΔT just after the shear is stopped. The shear cell we used adjusts in temperature in less than 2 minutes. Consequently, we cannot access to the influence of the temperature on the first relaxation but we can study the second relaxation process on always similar onions (same size and same compression). It enables us to study systematically the effect of the working temperature on the swelling kinetics.

We display in Figure 6 the temporal evolution of the reduced elastic modulus $G'(t) - G'(\infty)$ (where $G'(\infty)$ is determined by a simple fit) for two different temperatures. The semi-log scale shows that the kinetics is reasonably described by a single exponential whose characteristic time τ strongly depends upon T. The systematic study leads to Figure 7 where τ is plotted as a function of the working temperature. Apart from the fact that the characteristic time is essentially the same for the storage and the loss moduli, it can be seen that τ is strongly sensitive to the temperature: it varies from more than an order of magnitude when the temperature is raised from 20 to 30°C.

4 Analysis: a porous L_α phase

We now attempt to describe more quantitatively the kinetics. As already mentioned, it is characterized by a two-step relaxation from a rheological viewpoint. The first one leads to a rapid increase of the storage and loss moduli. Since the present measurements do not enable an accurate study of this first process, we defer it to a future work (by means of time-resolved X-ray scattering). Preliminary results already suggest that this initial stage is indeed highly non-linear and very complicated. However, it leads to a state of slightly compressed onions with a smectic period 10% smaller that the equilibrium value. The second stage is an exponential decrease of the elastic moduli. We assume that the second stage of the kinetics concerns the simple swelling of the onions (Fig. 8a) and we describe it by a diffusion model.

In a first step, we adopt a phenomenological approach: we assume that the swelling kinetics is driven by the balance of a restoring force originating from a slight compression of the membranes ($d < d_0$) against a viscous drag of the water flowing throughout the membranes (Stokes regime). The restoring force is described from the usual smectic free energy [23]. If u denotes the departure of the membrane position along the z-direction compared to the equilibrium position, the elastic stress (normal force per unit area) reads

$$\sigma_{\text{el.}} = d_0 \bar{B} \frac{\partial^2 u}{\partial z^2}\,, \tag{1}$$

where $\bar{B}$ is the compressiblity modulus of the L_α phase and we neglect the effect of bending deformations. (For systems stabilised by steric interactions, $\bar{B} = 9\pi^2(kT)^2/\kappa d_0^3$, with κ the rigidity of a single membrane [18]). The viscous drag is phenomenologically described using Darcy's equation. For a flow of water through a section of the L_α phase, the mean velocity reads [24]

$$\langle v \rangle = \frac{\mathcal{P}}{\eta_0} \nabla_z p\,, \tag{2}$$

where $\nabla_z p$ is the component of the pressure gradient along the direction of the membranes stacking, η_0 the viscosity of water and $\mathcal{P}$ the permeability of the L_α phase. From equations (1) and (2), one builds dimensionally the diffusion

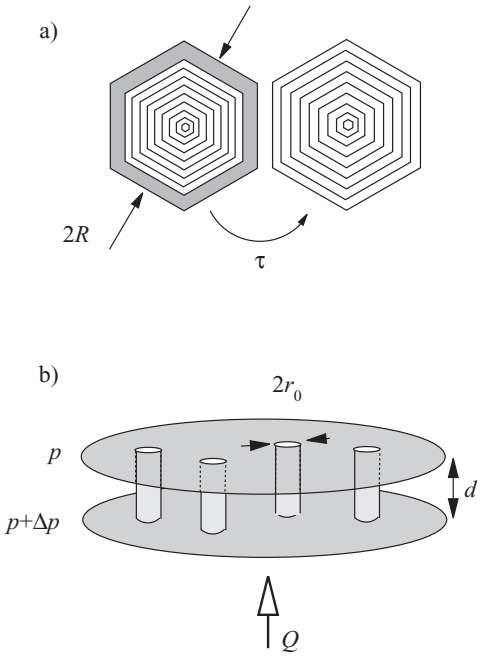

Fig. 8. (a) Schematic representation of the initial and final steps of the swelling kinetics (see Fig. 3). (b) Detail of the flow geometry: we assume that the water flows through channels connecting the membranes. For simplicity, these channels are considered cylindrical (radius r_0, height d_0) and dissipation takes place in those channels *via* a Poiseuille flow.

coefficient of the membranes displacement $D \sim \mathcal{P}\bar{B}/\eta_0$ which gives the relaxation time for the swelling kinetics:

$$\tau \sim \frac{\eta_0 R^2}{\mathcal{P}\bar{B}}\,, \tag{3}$$

by inserting as a characteristic spatial scale the onion lattice parameter R. According to this simple estimate, the swelling kinetics is entirely governed by the dependence of the permeability upon the temperature. The experimental results (Fig. 7) show that $\mathcal{P}$ increases of one order of magnitude when the temperature is raised by only 10°C.

The second step of our analysis consists in describing at a microscopic level the permeability of the lamellar phase. We assume that the flow of water is mediated by handle-like defects connecting neighbouring membranes (Fig. 8b). Such defects have been widely experimentally [25–27] and theoretically [28–31] studied. In particular, they appear to be precursors of the lamellar-to-sponge phase transition as a probable consequence of the evolution of the membrane elastic constants. We interpret the increase of the permeability as an increase of the defects density while raising the temperature closer to the sponge phase domain. For the sake of simplicity, we model these defects as simple cylinders (Fig. 8b) connecting two consecutive membranes, although their real shape is approximately a catenoid [26].

Assuming that the dissipation inside the cylinders is that of a Poiseuille flow, one obtains the permeability of the lamellar phase as a function of the surface density of

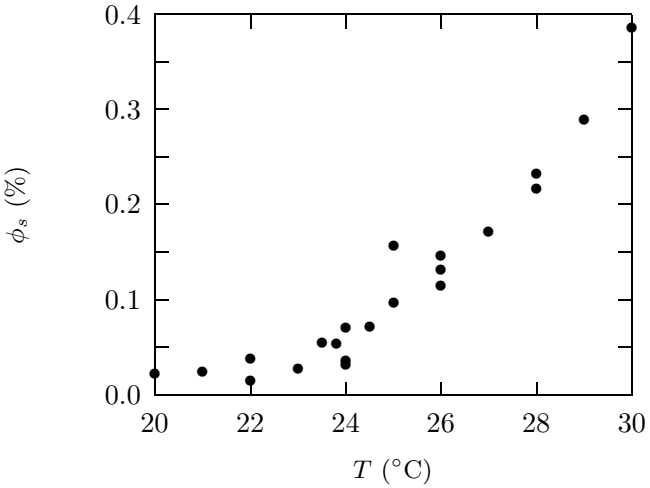

Fig. 9. Surface density of handle-like defects as a function of the working temperature according to equation (5). ($R = 10\,\mu$m, $d = 160$ Å, $\bar{B} = 300$ Pa, $\eta_0 = 10^{-3}$ Pa s, $r_0 = 0.5 d_0$.)

defects ϕ_s [24]

$$\mathcal{P} = \frac{r_0^2}{8}\phi_\mathrm{s}\,, \tag{4}$$

with r_0 the radius of one channel (Fig. 8b). Incorporating this result in equation (3), one obtains a link between the characteristic time of the swelling kinetics and the density of defects

$$\tau \approx \frac{\eta_0 R^2}{\bar{B} r_0^2 \phi_\mathrm{s}}\,. \tag{5}$$

This estimate is somehow speculative since it depends strongly on the geometry of the channels. For instance, τ is a function of r_0 which is *a priori* not well defined but certainly of order of d_0. Assuming $r_0 = d_0/2$, the Helfrich expression for $\bar{B}$ with $\kappa = 5 k_\mathrm{B} T$ [17], $R = 10\,\mu$m as given by light scattering, and the unknown numerical prefactor in equation (5) equal to 1 leads to figure 9. The surface density of defects increases sensibly with the temperature, although being small ($\phi_\mathrm{s} < 1\%$).

5 Conclusion

In this paper we consider the swelling kinetics of compressed multilamellar vesicles. This state corresponds to the stationary state of one particular L_α phase under a simple shear flow. The state of compression is evidenced by small-angle neutron scattering as well as by the optical observation of the sample under shear. It presumably results from the flow mechanism of the well-ordered texture of onions. Once the shear is stopped, the onion texture undergoes a relaxation kinetics leading to swollen onions that fill up the space. As probed by viscoelasticity, this kinetics exhibits a two-step process. The first step is not well time-resolved in the present experiment. In contrast, the second one is very slow and rheology is well suited to study the effect of the temperature on the kinetics. The combination of several observations strongly suggests

that this second stage directly concerns the swelling of the onions. This last process is faster and faster as the temperature is increased closer to the sponge phase domain. From the viscoelastic measurements, we deduce an estimate of the temperature-dependent permeability of the L_α phase. The second step of modelling the swelling kinetics consists in choosing a model for the permeability. We propose to attribute the increase of the permeability to the proliferation of handle-like defects connecting the membranes. The simplest model leads to an estimate of the density of defects per unit area. Results are in a good agreement with conductivity measurements on the same system [32] and in a qualitative agreement with various theoretical predictions [28–31]. However, the model we propose shows that the characteristic swelling time τ depends on experimental parameters that have not been systematically varied in the present work. We expect that τ varies as R^2, where R is the lattice parameter or as d_0, the equilibrium smectic period, from the combination $1/(\bar{B}r_0^2)$. This last parameter is indeed the easiest to vary since the range of lattice dimensions is very limited (10–20 μm). We, however, will study this effect in a future work as well as the early stage of the kinetics by using time-resolved X-ray scattering. Furthermore this model is very simple—probably over-simple—to describe correctly the short-time kinetics. One expects some reorganisation of the lamellar material at very short time (not described by the model) and indeed, time-resolved X-ray scattering shows a fairly complicated initial kinetics. However, we notice that the swelling kinetics offers a very convenient process to investigate the physical properties of membranes subjected to an external stress. A fair characterization of this kinetics is a prerequisite for further studies such as the dynamic of out-of-equilibrium membranes.

It is a real pleasure to thank A. Ajdari for helpful and numerous comments.

References

1. O. Diat, D. Roux, F. Nallet, J. Phys. France II **3**, 1427 (1993).
2. D. Roux, F. Nallet, O. Diat, Europhys. Lett. **24**, 53 (1993).
3. J. Bergenholtz, N.J. Wagner, Langmuir **12**, 3122 (1996).
4. J. Zipfel, J. Berghausen, P. Lindner, W. Richtering, J. Phys. Chem. B **103**, 2841 (1999).
5. J. Zipfel, P. Lindner, M. Tsianou, P. Alexandridis, W. Richtering, Langmuir **15**, 2599 (1999).
6. H. Hoffman, W. Ulbricht, Tenside Surf. Det. **35**, 421 (1998).
7. A. Alkahwaji, H. Kellay, Phys. Rev. Lett. **84**, 3075 (2000).
8. A. Leon, D. Bonn, J. Meunier, A. Alkahwaji, O. Greffier, H. Kellay, Phys. Rev. Lett. **84**, 1335 (2000).
9. A.G. Zilman, R. Granek, Eur. Phys. J. B **11**, 593 (1999).
10. A.S. Wunenburger, A. Colin, T. Colin, D. Roux, Eur. Phys. J. E **2**, 277 (2000).
11. L. Soubiran, C. Coulon, P. Sierro, D. Roux, Europhys. Lett. **31**, 243 (1995).
12. P. Panizza, D. Roux, V. Vuillaume, C.-Y.D. Lu, M.E. Cates, Langmuir **12**, 248 (1996).
13. O. Diat, D. Roux, F. Nallet, Phys. Rev. E **51**, 3296 (1995).
14. P. Sierro, D. Roux, Phys. Rev. Lett. **78**, 1496 (1997).
15. J. Penfold, E. Staples, I. Tucker, G.J.T. Tiddy, A.K. Lodi, J. Appl. Cryst. **30**, 744 (1997).
16. B.J. Ackerson, J.B. Hayter, N.A. Ackerson, L. Cotter, J. Chem. Phys. **84**, 2344 (1985).
17. P. Hervé, D. Roux, A.-M. Bellocq, F. Nallet, T. Gulik-Krzywicki, J. Phys. II **3**, 1255 (1993).
18. W. Helfrich, Z. Naturforsch. D **3**, 305 (1978).
19. J. Leng, P. Sierro, F. Nallet, D. Roux, O. Diat, in preparation.
20. W. Loose, B.J. Ackerson, J. Chem. Phys. **101**, 7211 (1994).
21. J. Leng, F. Nallet, unpublished small-angle neutron scattering data.
22. J. Leng, F. Nallet, D. Roux, O. Diat, P. Panine, unpublished X-ray scattering results.
23. F. Brochard, P.-G. De Gennes, Pramāna **1**, 1 (1975).
24. E. Guyon, J.-P. Hulin, L. Petit, *Hydrodynamique physique* (InterÉdtion/Édition du CNRS, 1994).
25. Ph. Bolthenhagen, M. Kléman, O.D. Lavrentovitch, J. Phys. II **4**, 1439 (1994).
26. X. Michalet, D. Bensimon, B. Fourcade, Phys. Rev. Lett. **72**, 168 (1994).
27. R. Strey, W. John, G. Porte, P. Bassereau, Langmuir **6**, 1635 (1990).
28. D.C. Morse, Phys. Rev. E. **50**, R2423 (1994).
29. L. Golubović, Phys. Rev. E. **50**, R2419 (1994).
30. G. Gompper, J. Goos, J. Phys. II **5**, 621 (1995).
31. T. Charitat, B. Fourcade, J. Phys. II **7**, 15 (1997).
32. L. Soubiran, *Mesures diélectriques de phases de membranes*, PhD thesis, University of Bordeaux-I (1996).